

NON-STOICHIOMETRY AND STRUCTURAL DISORDER IN SOME FAMILIES OF INORGANIC COMPOUNDS

Arne Magnéli

Arrhenius Laboratory, University of Stockholm, S-106 91 Stockholm, Sweden

Abstract - The structural background of non-stoichiometry in some families of inorganic compounds is discussed. The materials described include oxygen deficient tungsten trioxides at different degrees of reduction, and potassium intergrowth tungsten bronzes. The article stresses the importance of structural studies combining investigations by X-ray and electron diffraction and by electron-optical imaging.

INTRODUCTION

During the first decade of the 19th century one of the most intense controversies in the history of chemistry took place. The two combatants were French by birth - one Joseph Louis Proust being professor in Madrid and the other count Claude Berthollet holding a chair in Paris. It had become a generally accepted idea among chemists during the 18th century that a pure chemical compound has a constant composition. This was stated by Proust as a general law of constant proportions of a compound chemical species. The law was vigorously opposed by Berthollet who argued that the composition could vary within certain limits and depend on the conditions of formation. Hardly any experimental evidence to support either standpoint was presented, which is quite natural considering the state of the art of chemical analysis at the time. However, Proust became considered the winner of the fight as his view was generally accepted by the chemists. This outcome was largely due to the advent of Dalton's atomic theory, which so nicely seemed to explain the laws of constant and multiple proportions. These laws became the undisputed foundations for the science of stoichiometry. That chemical compounds could be non-stoichiometric, i.e. violate the law of constant proportions, was hardly considered possible by chemists for more than a century.

In 1914, however, the Russian chemist Kurnakov reported on results from studies of equilibria in binary metallic systems. He had found several instances of intermediary phases with compositions varying by several atomic percent of the components. He concluded from such observations that the stoichiometric compounds, which he called daltonides, may be looked upon as a special class of phases. Compounds of variable atomic composition - the non-stoichiometric compounds - form a more general class of phases, and Kurnakov called these berthollides.

Non-stoichiometry has since been found to be frequently occurring in non-molecular solid compounds. Kurnakov stated that this was a new, unexplored field of research giving promise of rich scientific progress, and this has certainly turned out to be true.

Research on non-stoichiometry has been conducted along various lines. Important results have been obtained with thermodynamic methods. Frenkel, Schottky and Wagner were among the pioneers in that field. The application of X-ray diffraction techniques gave the possibilities for crystallographic studies of the structural basis of non-stoichiometry. Among the several investigators who were active in such research, Hägg performed extensive studies on the mechanisms of non-stoichiometry in several groups of inorganic compounds, e.g. the sodium tungsten bronzes (Ref. 1). These materials were first prepared in the early nineteenth century by reduction of sodium polytungstates. The strange products with their extreme chemical inertness and beautiful colours ranging from glittering gold via red and purple to dark blue had attracted the interest of many chemists who tried to rationalize these materials as a series of distinct chemical compounds. Hägg by his X-ray powder diffraction investigations showed that this is rather an instance of an extraordinary wide range of non-stoichiometry.

Irrespective of the composition the crystal structure contains a three-dimensional framework made up of tungsten and oxygen atoms which are arranged as WO_6 octahedra mutually linked by corners (cf. Fig. 1). The big holes in the tungsten-oxygen skeleton are partially occupied by sodium atoms distributed at random. The occupancy may almost reach 100 percent, but also be as low as about 35 percent. The formula of this berthollide material may accordingly be

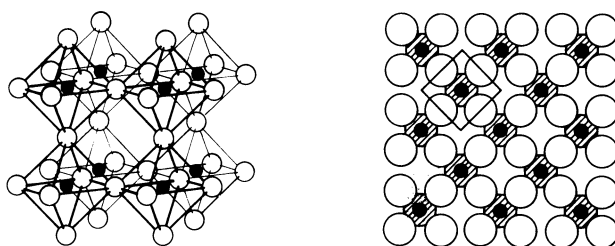


Fig. 1. The tungsten-oxygen network of the cubic sodium tungsten bronzes viewed in perspective and in projection along a cube axis.

written Na_xWO_3 with x values ranging from $1/3$ to unity. From the structural point of view the sodium tungsten bronzes may be looked upon as formed by addition of sodium atoms in a ReO_3 -type arrangement of WO_6 octahedra, i.e. in an idealized tungsten trioxide structure. Alternatively, they may be described as formed by subtraction of sodium atoms from an NaWO_3 structure of perovskite type.

STRUCTURE ANALYSIS BY X-RAY DIFFRACTION AND BY ELECTRON MICROSCOPY

Tungsten trioxide upon moderate reduction gives a dark blue product. The composition or formula of this product was, however, not well known; some investigators concluded from X-ray powder studies that the product is non-stoichiometric and that oxygen vacancies are likely to account for the deficiency in oxygen. A crystal structure investigation performed some 30 years ago, using X-ray diffraction data obtained from single crystals found in the blue reduction product, gave an entirely different result (Ref. 2).

The structure thus arrived at (Fig. 2) is rather like that of tungsten trioxide: the metal atoms have six oxygen neighbours octahedrally arranged and the WO_6 octahedra thus formed are mutually linked by corners as in the ReO_3 -type of structure. However, in the blue reduced oxide there are deviations from this simple pattern of linking. Some of the WO_6 octahedra share edges among themselves instead of corners, and the edge-sharing is arranged in such a way that groups of six octahedra are formed. Such groups of six edge-sharing octahedra are arranged at parallel planes extending through the crystal. The ReO_3 -type patterns

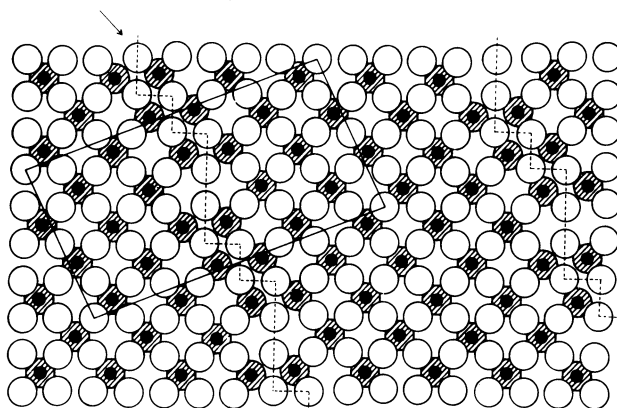


Fig. 2. Projection of the structure of $\text{W}_{20}\text{O}_{58}$ with dashed lines indicating edge-sharing between WO_6 octahedra at $\{103\}$ crystallographic shear planes and arrow showing direction of characteristic width of ReO_3 -type slabs ($n = 20 \text{WO}_6$ octahedra).

on each side of such planes are "out of phase" with respect to one another and this is the reason for the designation crystallographic shear (CS) later introduced to describe this phenomenon. The oxygen atoms which are engaged in edge-sharing at the shear planes are common to three WO_6 octahedra and thus account for the deficiency in oxygen compared to the WO_3 stoichiometry. The direction of the shear planes is $\{103\}$ with respect to the basic WO_3 structure.

The complete X-ray crystallographic structure determination directly gave the formula of the reduced oxide. It turned out to be $W_{20}O_{58}$, i.e. exactly $WO_{2.90}$. The reason why the formula is written $W_{20}O_{58}$ and not $W_{10}O_{29}$ is that 20 represents the number of WO_6 octahedra between two consecutive shear planes if the structure is viewed in the particular direction indicated in the figure.

The oxide studied in these experiments was prepared by heating mixtures of tungsten trioxide and tungsten dioxide in sealed tubes. Slight variations of the proportions of the starting materials did not lead to any shifts of the positions of the lines of the X-ray powder patterns of the products. This was taken as evidence that the $W_{20}O_{58}$ phase has a constant daltonide composition.

Results of X-ray structural studies of several binary molybdenum oxides and ternary molybdenum tungsten oxides of compositions lower in oxygen than trioxide stoichiometry are shown in Fig. 3 (Ref. 3 and 4). These phases contain crystallographic shear in a basic ReO_3 -type structure, but the edge-sharing takes place within groups of four octahedra instead of six as is the case in the $W_{20}O_{58}$ structure. The shear plane is $\{102\}$ in these structures whereas it is $\{103\}$ in the binary tungsten oxide.

The molybdenum oxides and the mixed molybdenum tungsten oxides form a series of analogously built structures, differing only with respect to the width of the ReO_3 -type slabs, which extend between the shear planes. The series of oxides comprises Mo_8O_{23} , Mo_9O_{26} , $(Mo,W)_{10}O_{29}$, $(Mo,W)_{11}O_{32}$ etc. The general formula of this "homologous" series of apparently daltonide

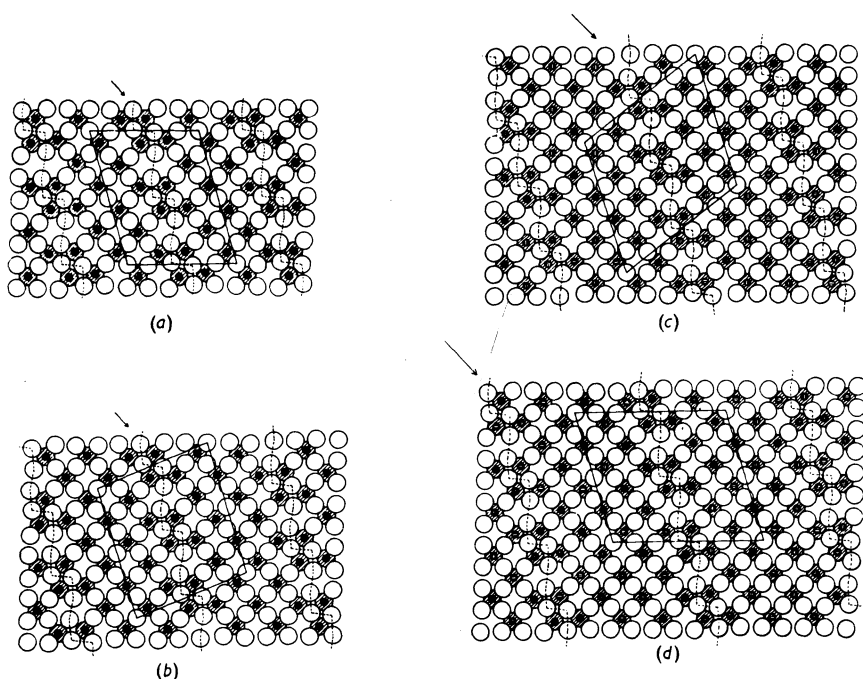


Fig. 3. Homologous series of molybdenum tungsten oxides M_nO_{3n-1} ($n = 8, 9, 10$ and 11) with $\{102\}$ crystallographic shear.

phases is M_nO_{3n-1} , where n with an observed maximum value of 14 represents the width of the slabs, i.e. the number of metal-oxygen octahedra between consecutive shear planes (Ref. 5).

Studies on other transition metal oxide systems such as titanium and vanadium oxides gave further evidence of the importance of crystallographic shear as a structural mechanism to accommodate a moderate reduction while still preserving the nearest coordination of oxygen around the metal atoms. These oxide systems were also found to contain long homologous series of daltonide phases.

For smaller degrees of reduction, i.e. for increasing distances between the shear planes, the difficulties to interpret the X-ray diffraction data were found to increase. It became evident that the structural problems set by such systems were approaching the limits of applicability of the X-ray techniques.

The way out of these difficulties was entered when Wadsley and others some ten years ago applied the electron microscope for lattice imaging of complex niobium oxides (Ref. 6). The availability of microscopes with a resolution of 3.5 Å or better and the advances in the theory of the image formation (Ref. 7 and 8) have helped to develop this technique into a means of imaging structures of crystals, applicable to large groups of chemical compounds.

In this connection it should be pointed out that the meaning of "structure" as obtained from electron microscope studies may differ considerably from that of X-ray diffraction structure. The single crystals used in X-ray experiments may seem very small, typically measuring thousandths or hundredths of a millimeter on an edge. This little volume, however, contains an enormous number of unit cells, and the crystal structure derived from the X-ray diffraction data represents an average structure of these unit cells, which individually may deviate more or less from the average. The image in the high resolution electron microscope shows the structure on the atomic level and is formed by a volume of the crystal which is less than the one used in the X-ray experiment by a factor of something like 10^{14} . The electron microscope is thus able to give detailed information about local deviations and defects in the crystal structure and also about local compositional variations.

ORDER AND DISORDER IN REDUCED TUNGSTEN TRIOXIDE

Reduced tungsten trioxide gives ample evidence of the applicability of electron microscopy for studies of non-stoichiometry and disorder. Research in that field has been reported by several authors in recent years. The present survey will mainly describe results obtained by M. Sundberg in investigations of samples of compositions $W_{3-x}O_8$ ($0 < x < 0.13$) mostly heated at temperatures above 1000°C for periods up to several weeks. The study, which was started as an attempt to prepare homologues of $W_{20}O_{58}$ and to determine structural characteristics of such phases, has since been considerably widened in its scope. The investigations of the reduced tungsten trioxide samples include characterization by X-ray powder photographs, single crystal X-ray structure determination whenever suitable crystals are obtained, and electron microscope studies involving electron diffraction and imaging of very thin crystal fragments.

An X-ray structure analysis of a single-crystal of a sample of approximately $W_{2.92}O_8$ composition had given a structure rather similar to that of $W_{20}O_{58}$ (Fig. 4a), with {103} crystallographic shear in a basic ReO_3 -type structure (Ref. 9). The difference lies in the thickness of the slabs between the shear planes. This corresponds to $n = 25$ WO_6 octahedra in the new phase, which gives the formula $W_{25}O_{73}$ ($W_{2.92}O_8$). The structure image is shown in the top picture of Fig. 4b. The texture of the areas between the dark dotted bands has the dimensions and orientation required by tungsten atoms arranged as in an ReO_3 -type structure.

These parts of the structure are obviously resolved. The dark bands are in an {103} orientation and comprise the groups of six tungsten atoms in edge-sharing octahedra. The tungsten atoms of the groups are not resolved but the interstices between them are visible. The micrograph thus gives a clear picture of the projection of the atomic arrangement in the direction of the electron beam.

However, a detailed analysis of the image shows that the spacing of the shear planes is not entirely uniform. The bottom picture of Fig. 4b is an interpretation of the area in the box in terms of WO_3 octahedra. Values of $n = 25$ are most frequent, but deviating n values are often found. The crystallite is thus not strictly stoichiometric in character and shows compositional deviations on the microlevel associated with variations in the thickness of the ReO_3 -type slabs (Wadsley defects).

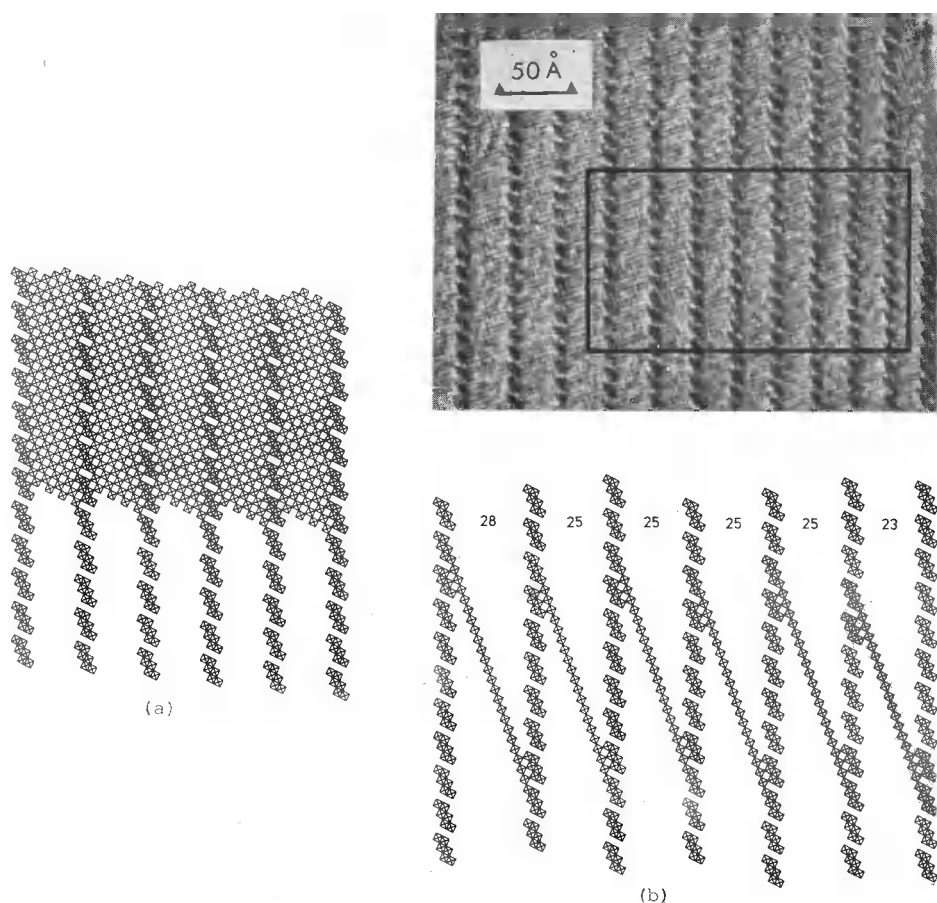


Fig. 4. Structure of $W_{20}O_{58}$ as formed by WO_6 octahedra (left). Structure of $W_{25}O_{73}$ (right). Top picture shows electron-optical image and bottom picture interpretation in terms of WO_6 octahedra of portion within box (Ref. 9).

The $W_{25}O_{73}$ structure is easily identified by the electron diffraction pattern shown in Fig. 5a. The substructure of ReO_3 -type is clearly visible, and the rows running in the $[103]$ direction, consisting of fairly sharp, weaker reflections at intervals of $1/25$ of the unit length in that direction, identify the crystallite as containing the $n = 25$ member of the W_nO_{3n-2} series. Electron diffraction studies of a large number of crystallites, however, show that some are characterized by n values other than 25, viz. in decreasing order of frequency 24, 23, 22 and 26. Some crystallites give diffraction patterns of two different n values, mostly 25 and 24 and should thus consist of $W_{25}O_{73}$ and $W_{24}O_{70}$ domains grown together in a coherent way.

The results obviously answer in the affirmative the question if homologues other than $W_{20}O_{58}$ exist in the series. However, it is also obvious that at higher n -values crystals of different homologues may form simultaneously and that there is a tendency towards compositional deviations by crystals containing Wadsley defects.

Crystallites from a sample of the composition $WO_{2.97}$ give a quite different diffractogram (Fig. 5b). It does not exhibit rows of fairly distinct spots in the $[103]$ direction but rather continuous streaks pointing in the $[102]$ direction. The structure image is shown in Fig. 6. The shear planes are in $\{102\}$ orientation, which means that edge-sharing takes place within groups of four WO_6 octahedra. The variation of the spacings between the shear

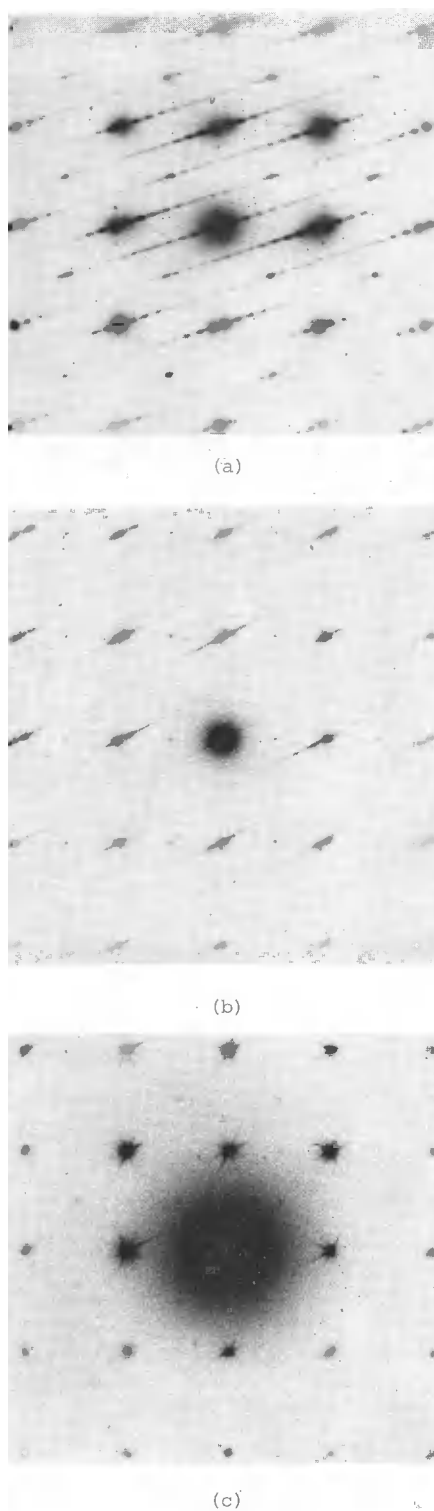


Fig. 5. Electron diffraction patterns of crystallites of compositions (from top) $WO_{2.92}$, $WO_{2.97}$ and $WO_{2.99}$ (Ref. 10).

planes is very large. The average n value for the crystal fragment ($n = 33-34$) gives an average composition of $WO_{2.97}$. The local compositional variations are considerable in spite of the long heating time at the synthesis. It seems appropriate to describe the material as substoichiometric berthollide tungsten trioxide. The deficiency in oxygen is associated with parallel but irregularly spaced crystallographic shear planes.

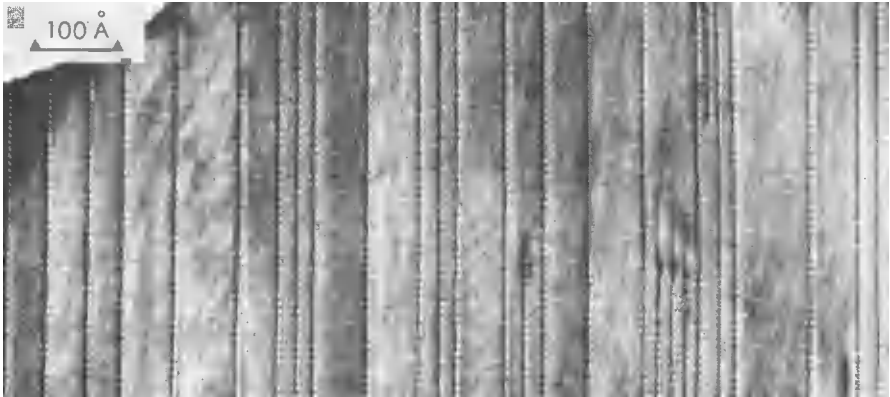


Fig. 6. Structure image of $WO_{2.97}$ crystallite. Shear planes ending within the crystal are likely to have formed under the influence of the electron beam in the microscope (Ref. 10).

For still smaller degrees of reduction the picture changes further. Fig. 5c gives the electron diffractogram of a crystallite of the approximate composition $WO_{2.99}$. The reflections are only those of tungsten trioxide but they show streaking by faint continuous rays protruding in all four equivalent directions $[102]$, $[201]$, $[\bar{1}02]$ and $[\bar{2}01]$. The structure image is shown in Fig. 7. It contains shear planes in all those four orientations with large and irregular spacings. It should be pointed out that tungsten trioxide, which is monoclinic at room temperature, is actually tetragonal at the temperature of formation of the reduced crystal. This may be the reason why shear planes appear with all possible orientations at small degrees of reduction. In this connection it is interesting to note that crystallographic shear in all orientations and with irregular spacing was observed by Gadó (12) in studies of the reduction of WO_3 to $W_{20}O_{58}$ at far-off-equilibrium conditions.

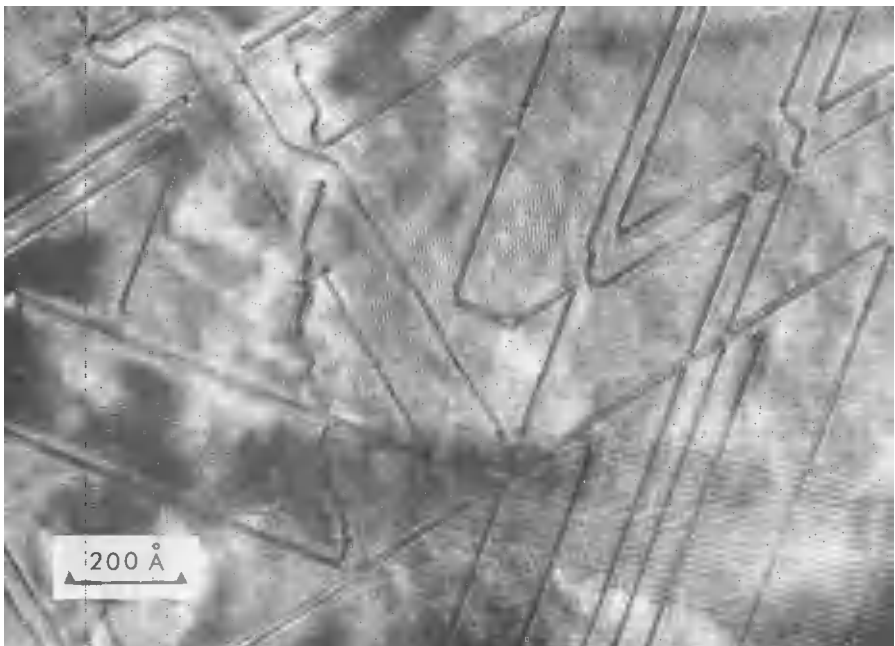


Fig. 7. Structure image of $WO_{2.99}$ crystallite (Ref. 11).

In conclusion it may be stated that the present knowledge of the mechanism of reduction in substoichiometric tungsten trioxide in its main lines is as follows: Slight reduction at elevated temperatures introduces crystallographic shear of {102} type in all possible directions and with irregular spacing. Further reduction suppresses all but one of the orientations of the shear planes, but they remain irregularly spaced and the nonstoichiometric character is preserved. Upon further reduction the shear planes change to an {103} orientation. This implies a higher reduction at the planes and serves to increase the spacing between them. As the reduction continues there is an increasing tendency of formation of discrete phases with narrow ranges of homogeneity and eventually phases approaching daltonide character.

Further experiments will be needed to add more detail to the picture of the structural mechanism of substoichiometry in tungsten trioxide. It may be mentioned that structure image studies have shown the transition from {102} to {103} crystallographic shear to be dependent not only on the degree of reduction but also on the temperature (Ref. 13).

INTERGROWTH TUNGSTEN BRONZES

For the alkali atoms larger than sodium, bronze structures occur which are different from the simple cubic structure referred to above. However, also these bronzes exist over considerable ranges of composition A_xW_3 and are instances of non-stoichiometry due to high concentrations of point defects. The hexagonal and tetragonal potassium tungsten bronzes illustrated in Fig. 8, both contain networks of WO_6 octahedra linked by corners. The tetragonal bronze structure contains pentagonal as well as square tunnels wherein the alkali atoms reside (Ref. 14). The potassium content may approach the theoretical upper limit of $K_{0.6}WO_3$, which corresponds to 100 percent occupancy of the sites in both types of tunnels. For lower x values the potassium atoms preferably occupy positions in the wider pentagonal tunnels (Ref. 15).

In the hexagonal bronze the potassium ions are situated within the wide six-sided tunnels formed by the WO_6 octahedra (Ref. 16) with average occupancies ranging from about 0.5 to unity. It has recently been shown (Ref. 8) that local variations in the potassium concentrations in the tunnels may be demonstrated by means of the lattice image technique.

A potassium tungsten bronze lower in alkali than the hexagonal phase has recently been found by Kihlberg and Hussain (Ref. 17). The new material which has been obtained within the compositional range K_xW_3 ($0.05 < x < 0.10$) (cf. Fig. 9) is described as an intergrowth tungsten bronze (ITB) for reasons to be presented in the following. It exhibits bronze characteristics such as metallic lustre, bluish black in colour, and chemical resistance towards attack by alkali solutions and strong acids.

The structural characterization of the new bronze was not made by X-rays but rather by means of electron diffraction and in particular electron-optical image techniques. Only at a later stage it was possible to obtain a suitable single crystal and to perform an X-ray structure analysis. This investigation fully confirmed the electron microscope results (and gave structural data of higher accuracy) (Ref. 17).

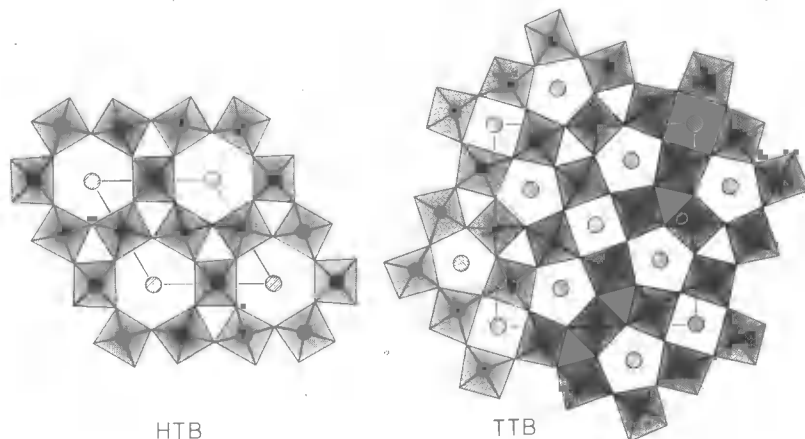


Fig. 8. Structures of hexagonal (HTB) and tetragonal (TTB) potassium tungsten bronzes.

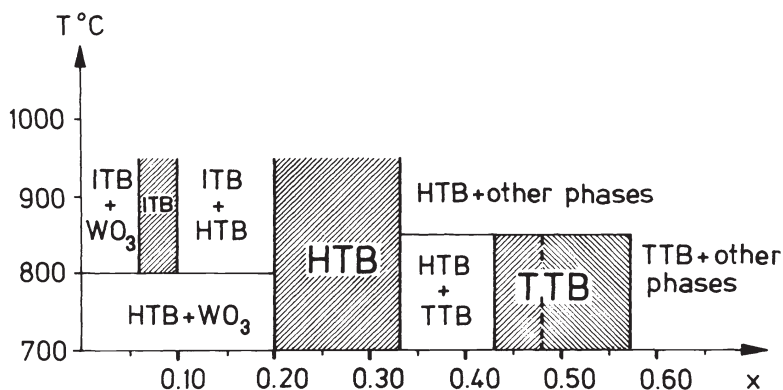


Fig. 9. Areas of formation of tetragonal (TTB), hexagonal (HTB) and intergrowth (ITB) tungsten bronzes in the K_xWO_3 system (Ref. 18).

The structure image of an ITB crystallite is given in Fig. 10. It is a very regular picture. The texture and dimensions of the lighter bands are in accordance with the tungsten atom arrangement in a resolved tungsten trioxide structure viewed along a pseudo-cube axis. The intermediary very marked double strings of "beads" may be interpreted as not entirely resolved tungsten atoms arranged in the same way as around the tunnels of the hexagonal tungsten bronze.

The resulting structure is illustrated in Fig. 11 in terms of WO_6 octahedra linked by corners. With potassium atoms occupying sites within the six-sided tunnels these should be approximately half-filled, which is roughly the same occupancy as in the hexagonal bronze at its minimum alkali content.

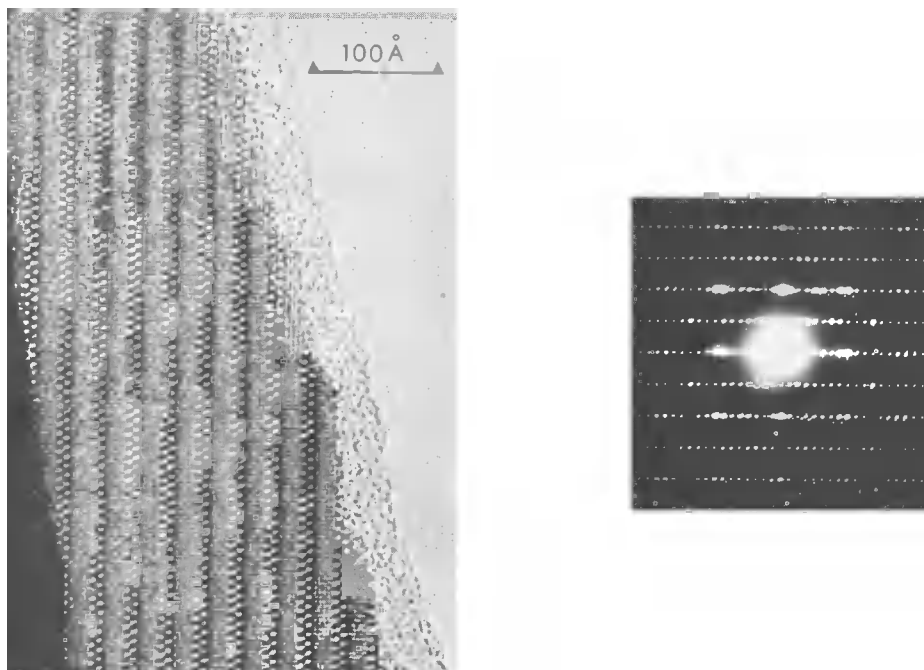


Fig. 10. Structure image and electron diffraction pattern of a crystallite of potassium intergrowth tungsten bronze.

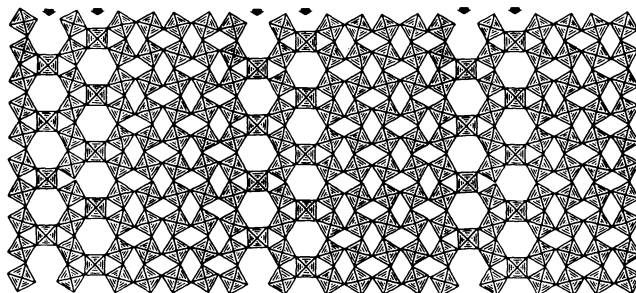


Fig. 11. Interpretation in terms of WO_6 octahedra of structure imaged in Fig. 10.

The structure may be described as an ordered intergrowth of slabs of hexagonal bronze type with slabs of distorted WO_3 type. The correctness of the structure has been confirmed by theoretical calculation of a synthetic electron microscope image from the structure model and, as mentioned above, also by a crystallographic structure determination based on single crystal X-ray data.

Families of analogous structures may be derived by changing the widths of the two types of slabs. Two of the structures in Fig. 12 also contain double rows of hexagonal tunnels but differ with respect to the thickness of the WO_3 slabs. Both types of structure have been identified in ITB samples by means of the electron microscope. As a matter of fact the very complicated X-ray powder patterns of the ITB preparations are completely accounted for if the sample is assumed to be a mixture of all three phases.

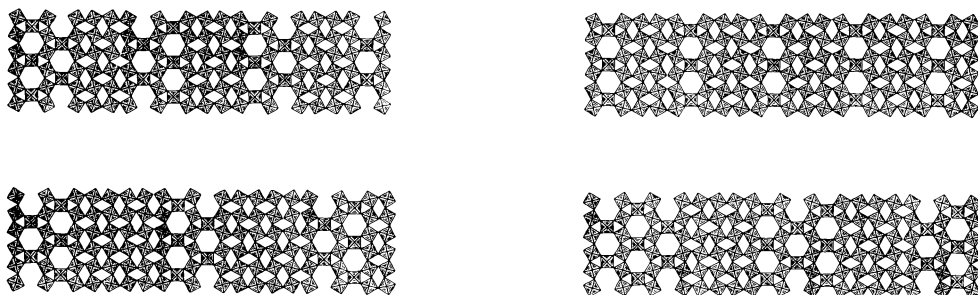


Fig. 12. ITB-type structures exhibiting different widths of WO_3 slabs (left) and of HTB slabs (right).

Structures deviating with regard to the widths of the hexagonal bronze slabs (cf. Fig. 12) have not been observed in ITB samples except as faults in structures of the type described above. The structure image of a crystallite of a rubidium intergrowth tungsten bronze (Fig. 13) shows a highly disordered structure with differing widths of the WO_3 slabs and instances of single as well as triple rows of hexagonal tunnels.

The combined studies by X-ray crystallography and electron microscopy techniques have shown that products formed within the ITB area of the diagram presented in Fig. 9 invariably are composite in character. The components are members of a series of closely related structures formed by an ordered intergrowth of slabs of WO_3 and HTB structure, the various members differing by the widths of the slabs. Attempts to prepare homogeneous samples of individual members of the series have so far been unsuccessful. The small crystals of the preparations, however, often contain just one type of structure with a moderate content of structural defects due to the local presence of slabs of deviating thickness. This suggests that the various structures form under similar conditions and once formed, a structure does not easily react to transform into a structural homologue.



Fig. 13. Image of disordered structure of rubidium intergrowth tungsten bronze.

The mechanism of non-stoichiometry in the intergrowth tungsten bronze structures is twofold. It evidently combines the features of extended defects, similar to the Wadsley defects, with gross point defects due to partial occupancy of the alkali atom positions in the hexagonal tunnels. Further research will be necessary to evaluate the combined effects on the non-stoichiometry of these two kinds of structural disorder.

CONCLUDING REMARKS

The instances of non-stoichiometry described above should serve to illustrate the importance of detailed structural knowledge for the appreciation of the often very intricate relations between daltonide and berthollide character in transition metal oxides. Structure image electron microscopy as a means to study structural defects and compositional variations on the atomic level has brought a most powerful complement to the structural knowledge obtainable with diffraction methods. The present rapid development of electron microscopes with higher resolution and the increasing insight in the theory of the image formation will certainly make the new technique applicable to further groups of compounds to provide knowledge of importance in correlating composition and structure with chemical and physical properties of materials.

REFERENCES

1. G. Hägg, *Z. Phys. Chem.* **B29**, 192-204 (1935).
2. A. Magnéli, *Arkiv Kemi* **1**, 513-523 (1949).
3. A. Magnéli, *Acta Chem. Scand.* **2**, 501-517 (1948).
4. B. Blomberg, L. Kihlborg and A. Magnéli, *Arkiv Kemi* **6**, 133-138 (1953).
5. A. Magnéli, *Acta Cryst.* **6**, 495-500 (1953).
6. J.G. Allpress, J.V. Sanders and A.D. Wadsley, *Acta Cryst.* **B25**, 1156-1164 (1969).
7. S. Iijima, *J. Appl. Phys.* **42**, 5891-5893 (1971).
8. J.M. Cowley and S. Iijima, *Phys. Today*, March, 32-40 (1977).
9. M. Sundberg, *Acta Cryst.* **B32**, 2144-2149 (1976).
10. M. Sundberg. Unpublished results.
11. L. Kihlborg and M. Sundberg, *Siemens Rev.* **43**, 3-8 (1976).
12. P. Gadó, *Acta Cryst.* **A16**, 182 (1963).
13. M. Sundberg and R.J.D. Tilley, *J. Solid State Chem.* **11**, 150-160 (1974).
14. A. Magnéli, *Arkiv Kemi* **1**, 213-221 (1949).
15. L. Kihlborg and A. Klug, *Chemica Scr.* **3**, 207-211 (1973).
16. A. Magnéli, *Acta Chem. Scand.* **7**, 315-324 (1953).
17. A. Hussain and L. Kihlborg, *Acta Cryst.* **A32**, 551-557 (1976).
18. A. Hussain and L. Kihlborg. Unpublished results.